

Generation and Detection of Coherent Optical Phonons in Germanium

T. Pfeifer, W. Kütt, and H. Kurz

Institute of Semiconductor Electronics, Rheinisch-Westfälische Technische Hochschule Aachen, D-5100 Aachen, Germany

R. Scholz

Institute for Theoretical Physics, Rheinisch-Westfälische Technische Hochschule Aachen, D-5100 Aachen, Germany

(Received 5 August 1992)

Coherent optical phonons are generated impulsively in Ge by irradiation with femtosecond laser pulses. They are detected via reflectivity modulations in the time domain in a pump-probe configuration. The deformation potential of the optical phonon is responsible both for the generation and for the detection process. The excitation of the coherent optical phonons is explained by anisotropic weakening of bonding valence orbitals.

PACS numbers: 78.47.+p, 42.65.Re, 63.20.-e, 72.20.Ht

Impulsive excitation of coherent phonons has been observed recently in molecules [1-4], metals [5,6], superconductors [7,8], and semiconductors [8-10]. A variety of excitation mechanisms have been discussed such as impulsive stimulated Raman scattering (ISRS) [2], displacive excitation mechanisms (DECP) [6], and generation of LO phonons via ultrafast screening of longitudinal surface space-charge fields [10-12]. In the case of noncentrosymmetric III-V compounds coherent phonons are observed by electro-optic sampling of the longitudinal field carried by the LO phonons [10,12]. In this Letter, we report the first observation of time-resolved phonons in a centrosymmetric crystal. The selection rules of the generation and detection process of coherent phonons in Ge are studied in detail. By varying independently the polarization of the pump and the probe beam relative to the sample orientation, conclusive information on the excitation process is obtained.

Excitation and detection of coherent optical phonons are performed at room temperature with 2-eV colliding-pulse mode-locked laser pulses of 50-fs duration. In our time-resolved reflection measurements, the pump and probe beams are kept close to normal incidence. The weak probe pulse samples the reflectivity changes induced by the intense pump pulse. Both beams are focused to a spot diameter of 14 μm . The excitation energy is approximately 150 pJ/pulse, leading to a density of photoexcited electron-hole pairs in the range of $(1-3) \times 10^{19} \text{ cm}^{-3}$. The time delay between probe and pump pulse is varied using a shaker-scanner system producing a maximum delay of approximately 4 ps at a scan frequency of 150 Hz. Signal averaging over 10^5 successive scans is accomplished directly with a high-speed computer system [13]. Alternatively, a stepper-motor driven delay stage is used as an optical delay, while the shaker scans a narrow window of 25 fs with 600 Hz, employing phase-sensitive lock-in detection. This setup allows the direct measurement of the time derivative of the reflectivity change $\partial(\Delta R)/\partial t$ [3,12].

Figure 1 shows the transient reflectivity change of a

(001)-oriented Ge sample. The polarization of the pump beam is set parallel to the (110) crystal axis, while the probe beam is orthogonally polarized to minimize coherent artifacts. The optical creation of the electron-hole pairs leads to a decrease in reflectivity. A simple Drude model is sufficient to explain the time-resolved reflectivity measurements [14]. Close examination of the reflectivity data in Fig. 1 reveals minute oscillations of less than $\Delta R/R_0 = 10^{-6}$, superimposed on the plasma-induced reflectivity change.

A time-derivative technique is employed to enhance the oscillations. Figure 2 shows experimental results obtained at fixed orthogonal polarization of the pump and probe pulses (i.e., $\varphi_{\text{pr}} = \varphi_{\text{pu}} - 90^\circ$) as a function of the sample orientation φ_s . The angle between the polarization of the pump pulse and the (100) crystal axis is $\varphi_{\text{pu}} \equiv \varphi_s$. For $\varphi_{\text{pu}} = \varphi_s = \pm 45^\circ$, i.e., when the pump field is parallel to (110) and $(1\bar{1}0)$, respectively, periodic oscillations are clearly visible. The phase of the coherent oscillations is the same for both orientations. For $\varphi_{\text{pu}} = 0^\circ$ and $\varphi_{\text{pu}} = 90^\circ$, however, i.e., for polarization along (100)

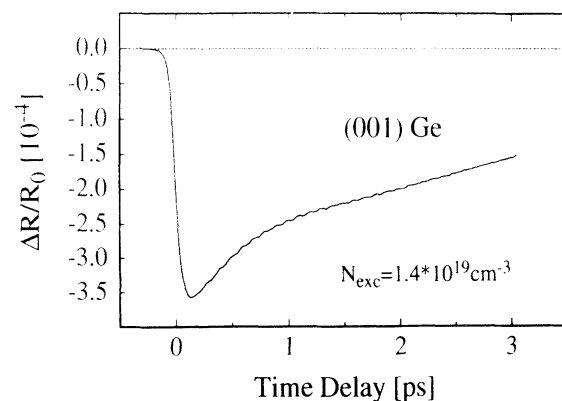


FIG. 1. Time-resolved change in the reflectivity of (001)-oriented Ge after excitation with a 50-fs, 2-eV laser pulse. The pump pulse is polarized along the (110) axis, orthogonal to the polarization of the probe pulse.

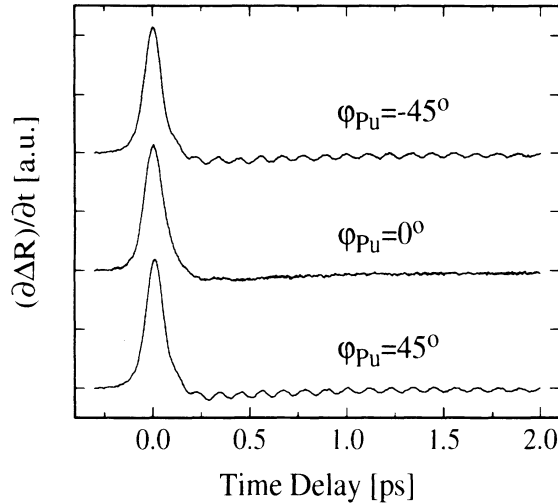


FIG. 2. Experimentally determined time derivatives of the transient reflectivity changes under orthogonal polarization for different sample orientations φ_s . $\varphi_{pu} \equiv \varphi_s$ is the angle between the (100) axis and the polarization of the pump beam.

and (010), the oscillations disappear completely. At fixed orthogonal pump and probe beams a $\sin^2(2\varphi_s)$ dependence in the amplitude of the phonon is observed.

Experiments with fixed orthogonal polarizations do not allow conclusive determination of whether the excitation or the detection process defines the selection rule for the appearance of coherent phonons. To clarify this point, the orientations of the pump and probe polarizations have been changed independently at fixed sample orientation. We start again with orthogonal polarizations, i.e., $\varphi_{pr} = -45^\circ$ and $\varphi_{pu} = 45^\circ$, which reproduces the results of Fig. 2. The oscillations in the reflectivity vanish completely, however, for $\varphi_{pr} = 0^\circ$ (φ_{pu} fixed at 45°) and $\varphi_{pu} = 0^\circ$ (φ_{pr} fixed at -45°).

The remaining question is whether a phase change of π occurs in the oscillations by rotating from $\varphi_{pr} = -45^\circ$ to $\varphi_{pr} = +45^\circ$ (at fixed $\varphi_{pu} = 45^\circ$). To solve this question, the pump beam polarization is again set along the $\varphi_{pu} = 45^\circ$ orientation, while the probe pulse is polarized along $\varphi_{pr} = 0^\circ$. The reflected probe beam is split via a polarizing beam splitter into $\varphi_{pr} = 45^\circ$ and $\varphi_{pr} = -45^\circ$ components and the difference of the reflected signals along $\varphi_{pr} = 45^\circ$ and $\varphi_{pr} = -45^\circ$ is recorded as a function of delay. The obvious large oscillations in Fig. 3 demonstrate that the detection of the phonon-induced oscillations scales with $\sin(2\varphi_{pr})$. The extremely high signal-to-noise ratio achievable in this reflective electro-optic sampling (REOS) technique [10,12] is due to the fact that no external reference pulse is used as a calibration. Just the difference of the two orthogonal components of the same reflected probe signal is recorded directly via a polarizing beam splitter. Applying this technique to centrosymmetric crystals like Ge, potential interactions become observable directly in the time domain as shown in Fig. 3.

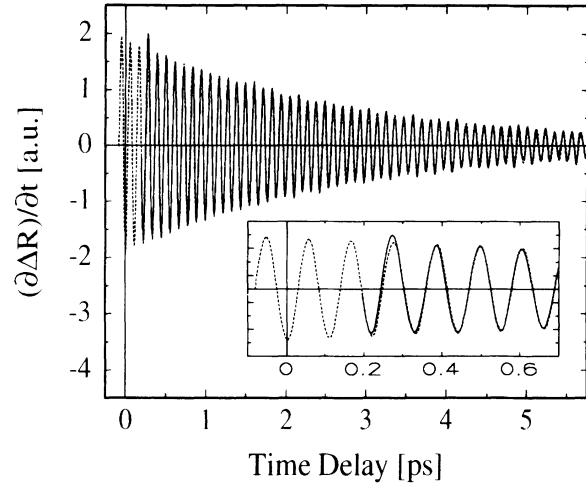


FIG. 3. Experimentally determined time derivative of the oscillatory parts (solid line) isolated from the background. The dashed curve shows a fit to the measured data, exhibiting a sine behavior around time delay $\Delta t = 0$ and a monoexponential decay with $T_2 = 2.7$ ps.

These experimental details are sufficient to explain the symmetry of the excitation process completely. With a $\sin(2\varphi_{pr})$ dependence of the detection process, a $\sin(2\varphi_{pu})$ dependence on the pump polarization has to be inferred to explain the $\sin^2(2\varphi_s)$ behavior observed at fixed orthogonal polarizations. Thus, a fourfold symmetry in the polarization of the pump beam is found under which coherent phonons appear in the reflectivity signature.

In order to eliminate the “slowly varying” signal component related to the free-carrier plasma, a smoothing algorithm is applied to the transient reflectivity data in Figs. 2 and 3. The smoothed curve is then subtracted from the actual data to isolate the oscillatory component. The resulting curve can be fitted by an expression for damped oscillations,

$$\partial(\Delta R)/\partial t = -Ae^{-t/T_2} \cos[\omega_0(t-t_0)], \quad (1)$$

where ω_0 is the phonon frequency, T_2 the phase relaxation time of the coherent optical phonons, and $\beta = \omega_0 t_0$ a phase shift referring to a reference time which is taken at the maximum of the anisotropic reflectivity change ΔR . With $T_2 = 2.707 \pm 0.030$ ps and $\beta = -5.33^\circ \pm 0.41^\circ$ the experimental data can be perfectly fitted. The frequency $\omega_0 = 9.086 \pm 0.001$ THz matches the Γ_{25} LO and TO phonon modes at $k = 0$. Integrating the time derivative $\partial(\Delta R)/\partial t$, we obtain a damped sine for the reflectivity ΔR itself, with a phase shift of less than 2 fs to positive times. The sine behavior points towards a ground-state excitation as the driving force.

The optical excitation of coherent phonons in Ge can be illustrated by a simple physical picture. During the pump pulse the carriers are anisotropically distributed in k space [15–17]. Each Ge atom has four next neighbors in the tetrahedral configuration. Valence orbitals be-

tween next neighbors are bonding, while conduction orbitals are antibonding. The excitation of electron-hole pairs weakens the strength of bonding. As long as the hole distribution is anisotropic in k space, the weakening is oriented preferentially. Two of the bonds form an angle of 35° with the (110) direction, while they are orthogonal on the $(\bar{1}\bar{1}0)$ direction; for the other two bonds, the reverse is true. When the polarization of the pump pulse is along (110), i.e., $\varphi_{pu} = 45^\circ$, the holes are excited mainly from one of these groups of bonds. For each reference atom, the strength of the bonds pointing to the (001) surface is different from the strength of the bonds pointing backwards. Because of this difference and the compensation of the bonds in the other Cartesian directions, the net driving force for the atoms is along the z axis. From femtosecond optical experiments on semiconductors and model calculations it is known that anisotropic carrier distributions relax much faster than the duration of excitation (50 fs) [16]. The lifetime of the anisotropic carrier distribution is shorter than half the period of an optical phonon, setting up a coherent optical lattice vibration along the z axis. If the pump polarization is turned from (110) to $(\bar{1}\bar{1}0)$, i.e., from $\varphi_{pu} = 45^\circ$ to $\varphi_{pu} = -45^\circ$, the roles of the bonds interchange. This results in a sign reversal of the initial driving force of the oscillation. A phase change of π is predicted, as observed in the experiments.

The coherent vibrations modulate the bond lengths, which implies a change of the valence-band energies and wave functions. As a result of this modulation, the coupling strengths and the transition frequencies of the resonances will change, leading to a modulation of the dielectric function. In our experiments, the modulation in the dielectric function is probed by measuring the change in reflectivity of a probe pulse at 2 eV. The symmetry of the phonon-induced modulation of the dielectric function is determined by the orientation of the Ge bonds in a tetrahedral configuration. In the x - y plane, the main axes of this anisotropy correspond to the projections of the Ge bonds on this plane. This anisotropy is observed in our experiment as an angular dependence of the reflectivity proportional to $\sin(2\varphi_{pr})$.

From a formal theoretical point of view the driving force arises from the anisotropic parts of the hole distributions, which are weighted with the deformation potential of the optical phonons. The selection rules are determined by the product of two interband dipole matrix elements and the phonon deformation potential [18], leading to a $\sin(2\varphi_{pu})$ behavior as derived from the intuitive picture above. Because the symmetry elements involved in the detection process are the same as in the excitation, we observe a similar angular dependence on the pump and probe polarization [18]. Even without explaining the full density matrix formalism here, we would like to stress that the detection can be understood in terms of Raman-like interband transitions only, while the excitation of

coherent oscillations requires short-lived anisotropic hole distributions [18].

The "sudden" excitation of anisotropic hole distribution has to be distinguished clearly from the generation of nonequilibrium incoherent phonons through the relaxation of hot electrons and holes. These nonequilibrium phonons are created within 3–4 ps in time-resolved experiments with ultrashort excitation pulses [19].

The strong hole-phonon coupling underlying the driving of coherent phonons in Ge governs vice versa the dephasing of coherent phonons as described in Eq. (1). At an excitation level of $N_e = N_h = 3 \times 10^{19} \text{ cm}^{-3}$, the decay of the phonon-induced reflectivity change within $T_2 = 2.7$ ps compares favorably with Raman linewidths of p -doped Ge. The dephasing time T_2 derived from Raman linewidths drops from the value of 3.8 ps for undoped Ge to 2.6 ps for heavily p -doped ($2 \times 10^{19} \text{ cm}^{-3}$) Ge, while n -type doping does not affect the linewidths significantly [20]. This close agreement confirms further the essential role of holes in destroying the phase of coherent optical phonons.

In recent time-resolved Raman experiments the temporal evolution of the population of nonequilibrium incoherent optical phonons in intrinsic Ge has been sampled [21,22]. Because of the limitations of time resolution, inherent in time-resolved incoherent anti-Stokes Raman experiments, the decay of optical phonons can only be evaluated with some ambiguity at room temperature. These experiments monitor the temporal evolution of the population of incoherent phonons, but do not directly reveal the population decay as pointed out very clearly in [19]. At room temperature the phonon population occurs within $T_p = 4$ –5 ps [21,22]. The actual decay time T_1 of phonons can be derived with $T_p = T_1 + T_g$, where T_g is the exponential generation time. With $T_g = 3.5$ ps as reported in the literature [19], T_1 is estimated to 1–2 ps. At moderate excitation densities ($\approx 10^{17} \text{ cm}^{-3}$), this decay time agrees very well with the data evaluated from Raman linewidths in intrinsic Ge ($T_2 = 3.8$ ps) [20], where the relation $T_2 = 2T_1$ remains valid.

Our experiments on dephasing of coherent optical phonons in the presence of a dense electron-hole plasma ($T_2 = 2.7$ ps at $N_e = N_h = 3 \times 10^{19} \text{ cm}^{-3}$), however, provide firm data on the reduction of T_2 through phonon-hole interactions down to time scales not accessible to time-resolved Raman experiments.

The generation of coherent optical phonons in (001)-oriented Ge with ultrashort laser pulses has been studied in time-resolved reflectivity experiments under various polarization conditions. The amplitude and phase of the coherent optical phonons in Ge are determined through the formation of anisotropic hole distributions in k space, which lead to a preferential weakening of bonding orbitals. The dephasing of optical phonons is strongly determined by interaction with photoexcited nonequilibrium holes.

We gratefully acknowledge helpful discussions with A. Stahl, H. J. Bakker, and K. Leo. We thank G. Maidorn for confirming experimental data on polarization dependence and A. Esser for the first experimental demonstration of coherent phonons in Ge. This work was entirely supported by the "Deutsche Forschungsgemeinschaft" and the "Alfried Krupp" Foundation.

-
- [1] M. J. Rosker, F. W. Wise, and C. L. Tang, *Phys. Rev. Lett.* **57**, 321 (1986).
- [2] Y. X. Yan and K. A. Nelson, *J. Chem. Phys.* **87**, 6240 (1987).
- [3] J. Chesnoy and A. Mokhtari, *Phys. Rev. A* **38**, 3566 (1988); *Rev. Phys. Appl.* **22**, 1743 (1987).
- [4] I. A. Walmsley, F. W. Wise, and C. L. Tang, *Chem. Phys. Lett.* **154**, 315 (1989).
- [5] T. K. Cheng, S. D. Brorson, A. S. Kazeroonian, J. S. Moodera, G. Dresselhaus, M. S. Dresselhaus, and E. P. Ippen, *Appl. Phys. Lett.* **57**, 1004 (1990).
- [6] T. K. Cheng, J. Vidal, H. J. Zeiger, G. Dresselhaus, M. S. Dresselhaus, and E. P. Ippen, *Appl. Phys. Lett.* **59**, 1923 (1991).
- [7] J. M. Chwalek, C. Uher, J. F. Whitaker, G. A. Mourou, and J. A. Agostinelli, *Appl. Phys. Lett.* **58**, 980 (1991).
- [8] W. Kütt, W. Albrecht, and H. Kurz, *IEEE J. Quantum Electron.* **28**, 2434 (1992).
- [9] K. Seibert, H. Heesel, T. Albrecht, J. Geurts, K. Allakhverdiev, and H. Kurz, in *Proceedings of the International Conference on Physics in Semiconductors*, edited by E. M. Anastassakis and J. D. Joannopoulos (World Scientific, Singapore, 1990), Vol. 3, p. 1981.
- [10] G. C. Cho, W. Kütt, and H. Kurz, *Phys. Rev. Lett.* **65**, 764 (1990).
- [11] R. Scholz and A. Stahl, *Phys. Status Solidi (b)* **168**, 123-138 (1991).
- [12] T. Pfeifer, T. Dekorsy, W. Kütt, and H. Kurz (to be published).
- [13] M. Strahnen, W. Kütt, and H. Kurz, in *Proceedings of an International Conference on VME-bus in Research*, edited by C. Eck (North-Holland, Amsterdam, 1988), p. 69.
- [14] A. Othonos, M. M. van Driel, J. Young, and P. Kelly, *Phys. Rev. B* **43**, 6682 (1991).
- [15] A. L. Smirl, J. R. Lindle, and S. C. Moss, *Phys. Rev. B* **18**, 5489 (1978).
- [16] R. Scholz and A. Stahl, *Phys. Status Solidi (b)* **173**, 199 (1992).
- [17] A. J. Taylor, D. J. Erskine, and C. L. Tang, *J. Opt. Soc. Am. B* **2**, 663 (1985).
- [18] R. Scholz, T. Pfeifer, and H. Kurz (to be published).
- [19] H. D. Fuchs, C. H. Grein, R. I. Devlen, J. Kuhl, and M. Cardona, *Phys. Rev. B* **44**, 8633 (1991).
- [20] F. Cerdeira and M. Cardona, *Phys. Rev. B* **5**, 1440 (1972).
- [21] F. Young, K. Wan, and H. M. van Driel, *Solid State Electron.* **31**, 455 (1988).
- [22] L. Ye, C. B. Roxlo, and A. Z. Genack, *Bull. Am. Phys. Soc.* **32**, 934 (1987); A. Z. Genack, L. Ye, and C. B. Roxlo, *Proc. SPIE Int. Soc. Opt. Eng.* **31**, 130 (1988).